

LA-UR-01-- 6492

Approved for public release;  
distribution is unlimited.

Title: Magnetotransport of the Low-Carrier Density One  
Dimensional  $s=1/2$  Antiferromagnet  $\text{Yb}_4\text{As}_3$

Author(s): P. Gegenwart, H. Aoki, T. Cichorek, J. Custers, M. Jaime, A.  
Ochiai, F. Steglich

Submitted to: International Symposium on Advances in Superconductivity  
and Magnetism, September 25-28, Mangalore, India



## Los Alamos

NATIONAL LABORATORY

Los Alamos National Laboratory, an affirmative action/equal opportunity employer, is operated by the University of California for the U.S. Department of Energy under contract W-7405-ENG-36. By acceptance of this article, the publisher recognizes that the U.S. Government retains a nonexclusive, royalty-free license to publish or reproduce the published form of this contribution, or to allow others to do so, for U.S. Government purposes. Los Alamos National Laboratory requests that the publisher identify this article as work performed under the auspices of the U.S. Department of Energy. Los Alamos National Laboratory strongly supports academic freedom and a researcher's right to publish; as an institution, however, the Laboratory does not endorse the viewpoint of a publication or guarantee its technical correctness.

## Magnetotransport of the low-carrier density onedimensional

$S=1/2$  antiferromagnet  $\text{Yb}_4\text{As}_3$

P. Gegenwart<sup>1</sup>, H. Aoki<sup>1</sup>, T. Cichorek<sup>1</sup>, J. Custers<sup>1</sup>, M. Jaime<sup>2</sup>, A. Ochiai<sup>3</sup> and F. Steglich<sup>1</sup>

<sup>1</sup>*Max-Planck Institute for Chemical Physics of Solids, D-01187 Dresden, Germany*

<sup>2</sup>*Los Alamos National Laboratory, Los Alamos, New Mexico 87545, USA*

<sup>3</sup>*Center for Low Temperature Science, Tohoku University, Sendai 980-8578, Japan*

### Abstract

The transport properties of the semimetallic quasi-one-dimensional  $S=1/2$  antiferromagnet  $\text{Yb}_4\text{As}_3$  have been studied by performing low-temperature ( $T \geq 0.02$  K) and high magnetic-field ( $B \leq 60$  T) measurements of the electrical resistivity  $\rho(T, B)$ . For  $T \geq 2$  K a “heavy-fermion” like behavior  $\Delta\rho(T) = AT^2$  with huge and nearly field-independent coefficient  $A \approx 3\mu\Omega\text{cm}/\text{K}^2$  is observed, whereas at lower temperatures  $\rho(T)$  deviates from this behavior and slightly increases to the lowest  $T$ . In  $B > 0$  and  $T \leq 6$  K the resistivity shows an anomalous magnetic-history dependence together with an unusual relaxation behavior. In the isothermal resistivity Shubnikov-de Haas oscillations, arising from a low-density system of mobile As-4p holes, with a frequency of 25 T have been recorded. From the  $T$ - and  $B$ -dependence of the SdH oscillations an effective carrier mass of  $(0.275 \pm 0.005)m_0$  and a charge-carrier mean-free path of 215 Å are determined. Furthermore in  $B \geq 15$  T the system is near the quantum limit and spin-splitting effects are observed.

PACS numbers: 71.27.+a, 75.10.Jm, 75.50.Ee

## 1) Introduction

The low-carrier density system  $\text{Yb}_4\text{As}_3$  has recently attracted the interest of many researchers due to its quantum-spin chains. At room temperature  $\text{Yb}_4\text{As}_3$ , crystallizing in the cubic anti- $\text{Th}_3\text{P}_4$  structure, is an intermediate-valent metal with an average valence ratio  $\text{Yb}^{3+}/\text{Yb}^{2+} = 1:3$  [1]. The Yb ions are located on the four interpenetrating families of the cubic space diagonals. At  $T_{\text{CO}} \approx 295$  K a charge-order (CO) transition, driven by intersite Coulomb repulsion and a deformation potential coupling to the lattice, takes place which causes the smaller  $\text{Yb}^{3+}$  ions to order along *one* of the cubic space diagonals. The trigonal lattice distortion accompanying the CO transition usually results in the formation of a polydomain low- $T$  structure. A preferential orientation of the domains can be induced by the application of a small uniaxial pressure along one space diagonal prior to cooling through  $T_{\text{CO}}$ . The crystal-electric field (CEF) ground state of the  $\text{Yb}^{3+}$  ions can be described by an effective  $S=1/2$  doublet [2]. The  $\text{Yb}^{3+}$  chains are well separated from each other by nonmagnetic  $\text{Yb}^{2+}$  and As ions. The low-energy excitations of these  $S=1/2$  chains have been found using inelastic neutron-scattering (INS) experiments [2] to agree well with the des Cloizeaux-Pearson “magnon” spectrum (lower bound of the two-spinon continuum) of a  $S=1/2$  antiferromagnetic (AF) Heisenberg chain with a nearest-neighbor AF coupling  $|J| = 2.2$  meV (corresponding to  $k_B \cdot 25.5$  K). The large “heavy-fermion” (“HF”) like in- $T$  linear contribution to the specific heat,  $C(T)/T = \gamma$  with  $\gamma = 0.2$  J/K<sup>2</sup>mol [1], is in excellent agreement with the expected “magnon” contribution. The application of magnetic fields  $B$  with a finite component perpendicular to the spin chains leads to the opening of a gap  $\Delta(B)$  in the low-energy excitation spectrum and “soliton”-type anomalies, which were first observed in specific-heat [3], thermal-expansion and thermal-conductivity measurements [4]. The spin gap was later directly confirmed using inelastic neutron diffraction at the boundary of the AF Brillouin zone [5]. Below 12 T, a  $\Delta(B) \sim B^{2/3}$  dependence was observed [6] which

can be explained in the frame of the quantum sine-Gordon model taking into account an alternating Dzyaloshinskii-Moriya (DM) interaction [7]. Furthermore, at very low- $T$  a spin-glass (SG) transition at  $T_{\text{SG}} = 0.15$  K arises due to weak ferromagnetic interchain coupling and disorder [6,8]. A detailed review on the magnetic properties of  $\text{Yb}_4\text{As}_3$  is given in [9,10], and most recent results concerning the SG properties can be found in [6]. Here, we concentrate on the unusual electrical-transport properties of  $\text{Yb}_4\text{As}_3$ .

The  $4f$  electronic state in the CO state, which is slightly incomplete, can be expressed as  $\text{Yb}^{3+}\text{Yb}_3^{2+}\text{As}_3^{3-}$ , where the smaller  $\text{Yb}^{3+}$ -ions are arranged predominantly on the short chain parallel to, e.g., the former cubic  $\langle 111 \rangle$  direction. The low- $T$  Hall coefficient  $R_H$  is positive, implying a dominant hole conduction. The value of  $(eR_H)^{-1} = 7 \times 10^{13} \text{ cm}^{-3}$  corresponds to a density of only 0.001 per  $\text{Yb}^{3+}$ -ion, if one assumes the presence of only one type of charge carriers [1]. Non-spin-polarized LDA band-structure calculations of the hypothetical  $\text{LuYb}_3\text{As}_3$  system suggested a semimetallic character of  $\text{Yb}_4\text{As}_3$  [11]. Antonov et al. [12] calculated the LSDA+ $U$  band structure of  $\text{Yb}_4\text{As}_3$  for energies close to the Fermi level. The  $U$  value was adjusted to  $U_{\text{eff}}^{3+} = 9.6$  eV, and the  $f$  shell of the  $\text{Yb}^{3+}$  ions was treated as a core shell. An extremely narrow marginally occupied  $\text{Yb}^{3+}$ - $4f$  hole band was pinned, via the charge balance between Yb and As, at the top of the As- $4p$  valence band. Thus, the number of As- $p$  holes exactly equals the number of excess Yb- $4f$  electrons in the partially filled  $4f$  hole level. Therefore, the Fermi surface consists of (1) a hole pocket of light ( $\sim 0.6m_0$ ) As- $4p$  states centered on the  $\Gamma$  point and (2) an electron pocket centered on the  $\Gamma$ -P symmetry line with a heavy effective mass of about  $38m_0$  [12]. The mobility of these heavy  $4f$  electrons is almost negligible compared to that of the light As- $4p$  holes.

Most remarkably, the electrical resistivity  $\rho(T)$  was reported to follow a  $T^2$  behavior between 2 and 40 K, with a giant coefficient  $A \approx 0.75 \text{ } \mu\Omega\text{cm/K}^2$  [1]. The Kadowaki-Woods scaling

observed for usual HF metals is fulfilled (within a factor of 2), although the low-carrier concentration excludes the usual Kondo effect to be operating.

This article is organized as follows: After giving details concerning experimental techniques in the next section, we address in section 3 the yet unexplained “HF” behavior in  $\rho(T)$ . In section 4 we present new results on unusual hysteresis and relaxation which were found for  $B > 0$  in the electrical resistivity. A quantitative analysis of Shubnikov-de Haas (SdH) oscillations observed in the isothermal resistivity is given in section 5, and the summary is presented in section 6.

## 2) Experimental details

The experiments were performed on rectangular pieces, approximately  $(1.8 \times 0.7 \times 0.3)$  mm<sup>3</sup>, of a high-quality single crystal that was grown by a self-flux method as described in [1]. The electrical resistivity  $\rho(T, B)$  was measured using the standard four-probe ac-method adapted to a <sup>3</sup>He/<sup>4</sup>He dilution refrigerator with a 19 T superconducting magnet. High-field experiments were performed in the Los Alamos High Magnetic Field Laboratory using a short pulse (25 msec) 60 T magnet.

## 3) “Heavy-fermion” behavior in resistivity

As shown in Fig. 1, part (a), the resistivity follows a  $\rho(T) - \rho_0 = AT^2$  dependence with  $A = 3.4$   $\mu\Omega\text{cm}/\text{K}^2$  down to 4 K. At lower temperatures,  $\rho(T)$  deviates from the  $T^2$  dependence, passes through a minimum at 2 K followed by an 0.15% increase which saturates below 0.1 K, see Fig. 1b. The increase of the resistivity below about 4 K might be related to spin-disorder scattering above the SG freezing which was observed in ac-susceptibility measurements below 0.15 K [6,8]. Alternatively, it might be ascribed to the dynamic character of the CO state, see below. Compared to the early measurement by Ochiai et al. [1], our recent experiments reveal roughly three times higher values both of the residual resistivity  $\rho_0$  and the

coefficient  $A$  as well as a more than two times larger Hall coefficient, corresponding to a carrier concentration  $(eR_H)^{-1} = 3 \times 10^{13} \text{ cm}^{-3}$  [9]. The large coefficient  $A$  is slightly increasing with  $B$ -fields up to 18 T [8], while the specific heat coefficient  $\gamma$  rapidly decreases indicating the formation of a spin gap in the “magnon” spectrum [3] (see Fig. 1c,d). This observation is in striking conflict with the assignment of the large  $A$  coefficient as resulting from the scattering of light carriers off the “magnon” excitations [12]. We, therefore, propose that in  $\text{Yb}_4\text{As}_3$  it is the scattering of light and mobile As-4p holes off the heavy Yb-4f electrons that leads to HF-type behavior in the resistivity. The band structure should not be affected by magnetic fields of the order of 10 T [13]. Therefore, the large  $A$  coefficient also remains almost constant and does not reflect the field-induced gap in the spin-excitation spectrum.

#### 4) Unusual relaxation behavior in $B > 0$

The isothermal resistivity roughly follows a  $B^2$  behavior (Fig. 2a), typical for compensated semimetals. The superimposed Shubnikov-de Haas oscillations will be discussed in the subsequent section. A pronounced hysteresis is observed upon increasing and decreasing  $B$  (Fig. 2a) as well as upon warming and cooling in  $B > 0$  [8]. This effect which has also been observed by Aoki et al. [14] occurs on monodomain  $\text{Yb}_4\text{As}_3$  as well [8]. The hysteretic behavior indicates a metastable state in  $B > 0$ . To further study this effect, we recorded the time ( $t$ ) dependence of the resistivity at 2 K after applying 16.5 T with a rate of 0.25 T/min (Fig. 2b) as well as after reducing the field back to 0 T with the same rate (Fig. 2c). The observed relaxation cannot be fitted by a simple logarithmic decay. Even 10 hours after switching off the field, no saturation occurs and as shown in Fig. 2c, the resistivity is still far from its value at the beginning of the measurements. The 30 T and 58 T pulsed-field experiments revealed that an increase of the maximum field increases the hysteresis between the  $\rho(B)$  curves, see below (Fig. 6a.). Upon increasing the temperature, the relaxation effect becomes gradually suppressed: Fig. 3 displays  $\rho(t)$  in 16.5 T at various temperatures. The

amplitude of the relaxation decreases with increasing  $T$  and vanishes for  $T \geq 7$  K. Following Aoki et al. [14] we tried to fit our  $\rho(t)$  data with the sum of two exponential decays, which works satisfactorily well above 2 K, but only very approximately at lower temperatures. The obtained two time constants  $\tau_1$  and  $\tau_2$  decrease continuously from below 7 K (inset Fig. 3). A more precise determination for  $\tau_2$  below about 2 K would require a registration of  $\rho(t)$  for more than 10 hours.

The observed relaxation and hysteresis might possibly indicate a slow thermally activated domain motion [15], i.e. either (i) the motion of chain domains related to the domain structure of our polydomain samples or (ii) the motion of magnetic domains related to the SG behavior below 0.15 K [8]. A motion of chain domains would result in a pronounced relaxation in the magnetization, too, because the low- $T$  susceptibility is strongly anisotropic [16]. However, as shown in Fig. 4, neither hysteresis nor relaxation was found in the dc-magnetization of polydomain  $\text{Yb}_4\text{As}_3$ . On the other hand, a motion of SG domains is unlikely, because the effect occurs well above  $T_{\text{SG}}$  and in very large magnetic fields (i.e. up to 58 T).

Another possibility is that the unusual relaxation is related to the slightly incomplete CO, being dynamic in nature (electron hopping via As-4p states between  $\text{Yb}^{3+}$  and  $\text{Yb}^{2+}$  nearest-neighbor sites on different space diagonals). Most interestingly, no similar hysteresis and relaxation occurs in the resistivity of the doped, but charge-ordered system  $\text{Yb}_4(\text{As}_{0.96}\text{Sb}_{0.06})_3$ . The latter is also lacking the low- $T$  increase in  $\rho(T)$  (Fig. 1b).

## 5) Shubnikov-de Haas oscillations

In the following we analyze the isothermal resistivity which shows SdH oscillations recently also observed by Aoki et al. [14]. The analysis is complicated by the hysteresis and relaxation effects discussed in the previous section. Only for measurements taken in decreasing field the positions of the SdH could be determined consistently for all temperatures up to 7 K. To

analyze the SdH frequency we used the field range  $4.5 \text{ T} \leq B \leq 12.5 \text{ T}$  (Fig. 5a). As shown in Fig. 5b, the oscillations result from the depopulation of the Landau tubes  $N = 4, 3$  and  $2$ . A SdH frequency  $F$  of  $25 \text{ T}$  is determined, in agreement with [14]. This most likely arises from the As-4p holes since their mobility is much higher than that of the Yb-4f electrons. Assuming one pair of As-4p bands as derived from LSDA+U band-structure calculations [12],  $F$  would correspond to a carrier concentration of  $n \approx 1.4 \times 10^{13} \text{ cm}^{-3}$ . This value, however, is about two times smaller than  $(eR_H)^{-1} \approx 3 \times 10^{13} \text{ cm}^{-3}$  determined for the same single crystal. The reason for this discrepancy is yet unclear and needs further theoretical investigations.

In a previous paper [8], the observation of two characteristic frequencies  $F_1 = (40 \pm 10) \text{ T}$  and  $F_2 = (112 \pm 5) \text{ T}$  has been reported. In these measurements, which were performed under uniaxial pressure along the cubic  $\langle 111 \rangle$  direction in order to induce a monodomain low- $T$  state, a sample with much larger cross section had to be used. Therefore, the sensitivity was much lower than in the measurements reported here. In [8], SdH oscillations had been visible only in the field interval  $10 \text{ T} \leq B \leq 18.8 \text{ T}$ . In this field range, however, as shown in Fig. 6, additional oscillations occur which now can be attributed to spin-splitting effects: due to the low-carrier concentration, the system is already in its quantum limit. Assuming a splitting  $\nu_s = 0.016 \text{ T}^{-1}$  of the  $N = 1$  maximum (see dotted lines in Fig. 6b, a very similar value was found also in [14]), the effective Landé  $g$ -factor for the As 4p holes given by  $g_{e,\pi} = 2F \nu_s / (m_{e,\pi}/m_0)$  is calculated to  $2.9 \pm 0.2$ . Here we used the value for the effective carrier mass  $m_{e,\pi} = (0.275 \pm 0.005)m_0$  determined from the analysis of the  $T$ -dependence of the SdH oscillations in low fields  $4.5 \text{ T} \leq B \leq 11 \text{ T}$  discussed below. A Fast-Fourier transformation of the data up to  $30 \text{ T}$  reveals a very similar spectrum as found in the early experiment on the monodomain sample [8] which proves that (i) there is no significant difference between the measurements on polydomain  $\text{Yb}_4\text{As}_3$  for  $B \parallel \langle 110 \rangle$  and monodomain  $\text{Yb}_4\text{As}_3$  for  $B \parallel \langle 111 \rangle$ , in agreement with the predicted almost spherical As-4p hole Fermi surface [12] and that (ii) the frequencies



$F_1$  and  $F_2$  do not represent the true SdH frequency, but are caused most likely by spin-splitting effects.

To determine the effective carrier mass related to the SdH frequency of 25 T, we used the  $T$  dependence of the SdH oscillations related to  $N = 4$  and  $N = 3$ , i.e. those detected below 10 T. At higher magnetic fields, the observed  $T$  dependence of the SdH oscillations could not be described well using the standard Lifshitz-Kosevich (LK) theory. This is caused by both the spin-splitting effects discussed above and the already discussed unusual hysteresis effects that strongly increase in size at higher  $B$  and lower  $T$ . Therefore, we have excluded measurements taken below 2 K from the mass analysis, too. As shown in Fig. 7a, the  $T$  dependence of the SdH oscillations can be well fitted by the LK theory. The resulting effective carrier mass  $m_{e\pi} = (0.275 \pm 0.005)m_0$  is smaller than that ( $0.4m_0$ ) obtained by Aoki et al. [14] from their analysis for SdH oscillations below 2 K. Most interestingly, both these values are substantially smaller than that of the cyclotron-resonance (CR) mass  $m_{CR} = 0.72m_0$  [17]. This is opposed to Kohn's theorem for electron motion in a Galilean invariant electron gas [18], according to which  $m_{CR}$ , originating from the center of mass motion of the electron system in a magnetic field, must be smaller than  $m_{e\pi}$ , since the latter only is affected also by electron-electron interactions. A similar violation of Kohn's theorem has been observed in the rare-earth monpnictides GdAs [19] and LaSb [20]. For both of these semimetallic systems,  $m_{CR}$  was found to be twice as large as the de Haas-van Alphen derived  $m_{e\pi}$ . As shown in a theoretical study of the cyclotron resonance by Kanki and Yamada [21], Umklapp processes may reduce the resonance frequency of non-interacting electrons leading to an *increase* in  $m_{CR}$ . According to their theory, Kohn's theorem is not necessarily valid for strongly correlated electron systems.

As shown in Fig. 7b, the analysis of the field dependence of the oscillations below 8.5 T taken at differing temperatures reveals a Dingle temperature of  $T_D = 6.6$  K, corresponding to a

charge-carrier mean-free path of  $\ell \approx 215 \text{ \AA}$ . We note that the magnon mean-free path along the  $S=1/2$  chains determined from the  $B = 0$  thermal conductivity is roughly  $500 \text{ \AA}$  [9], and that both values are much smaller than the domain size of approximately  $1 \text{ }\mu\text{m}$ .

## 6) Summary

The transport properties of the low-carrier density 1D  $S=1/2$  antiferromagnet  $\text{Yb}_2\text{As}_3$ , arising from its 3D semimetallic electronic band structure, were investigated down to very low temperatures ( $T \geq 20 \text{ mK}$ ) and up to very high magnetic fields ( $B \leq 60 \text{ T}$ ). The “HF” like resistivity observed even in high magnetic fields where the large  $B = 0$  in- $T$  linear specific heat is suppressed, suggests a two-band model of current-carrying As-derived  $4p$ -holes scattered by heavy Yb-derived  $4f$ -electrons. An unusual hysteresis was observed in the isothermal magnetoresistance indicating a metastable state in  $B > 0$ . A very slow relaxation of the resistivity could be detected for temperatures below  $7 \text{ K}$ . This effect can neither be related to chain-domain motion nor to SG domain motion, but seems to rather point to the slow motion of point defects due to the dynamic nature of the CO state. A detailed analysis of the isothermal resistivity reveals SdH oscillations with a very low frequency of  $25 \text{ T}$  which confirm the existence of a small concentration of light As- $4p$  holes. The effective carrier mass is estimated to  $m_{\text{eff}} = (0.275 \pm 0.005)m_0$ , a value more than two times smaller than the observed CR mass  $m_{\text{CR}} = 0.72m_0$  [17].

## Acknowledgements

Stimulating discussions with T. Suzuki, B. Schmidt, P. Thalmeier and A. Yaresko are gratefully acknowledged.

## References:

- [1] A. Ochiai, T. Suzuki, T. Kasuya, J. Phys. Soc. Jpn. 59 (1990) 4129.
- [2] M. Kohgi, K. Iwasa, J.-M. Mignot, A. Ochiai, T. Suzuki, Phys. Rev. B 56 (1997) R11388.
- [3] R. Helfrich, M. Köppen, M. Lang, F. Steglich, and A. Ochiai: J. Magn. Magn. Mat. 177-181 (1998) 309.
- [4] M. Köppen, M. Lang, R. Helfrich, F. Steglich, P. Thalmeier, B. Schmidt, B. Wand, D. Pankert, H. Benner, H. Aoki, and A. Ochiai: Phys. Rev. Lett. 82 (1999) 4548.
- [5] M. Kohgi, K. Iwasa, J.-M. Mignot, B. Fåk, P. Gegenwart, M. Lang, A. Ochiai, H. Aoki, and T. Suzuki: Phys. Rev. Lett. 86 (2001) 2439.
- [6] P. Gegenwart, H. Aoki, T. Cichorek, J. Custers, N. Harrison, M. Jaime, M. Lang, A. Ochiai and F. Steglich: Physica B (in press).
- [7] M. Oshikawa, K. Ueda, H. Aoki, A. Ochiai, and M. Kohgi: J. Phys. Soc. Jpn. 68 (1999) 3181.
- [8] P. Gegenwart, T. Cichorek, J. Custers, M. Lang, H. Aoki, A. Ochiai, and F. Steglich: J. Magn. Magn. Mat. 226-230 (2001) 630.
- [9] B. Schmidt, H. Aoki, T. Cichorek, J. Custers, P. Gegenwart, M. Kohgi, M. Lang, C. Langhammer, A. Ochiai, S. Paschen, F. Steglich, T. Suzuki, P. Thalmeier, B. Wand, and A. Yaresko: Physica B 300 (2001) 121.
- [10] B. Schmidt, H. Aoki, T. Cichorek, P. Gegenwart, A. Ochiai, and F. Steglich: J. Phys. Soc. Jpn. (in press).
- [11] H. Harima: J. Phys. Soc. Jpn. 67 (1998) 37.
- [12] V.N. Antonov, A.N. Yaresko, A.Ya. Perlov, P. Thalmeier, P. Fulde, P.M. Oppeneer, H. Eschrig: Phys. Rev. B 58 (1998) 975.
- [13] A.N. Yaresko, unpublished results.

- [14] H. Aoki, A. Ochiai, H. Aoki, N. Kimura, T. Terashima, C. Terakura, and H. Harima: J. Phys. Soc. Jpn., submitted.
- [15] T. Suzuki and H. Aoki, private communication.
- [16] H. Aoki, A. Ochiai, M. Oshikawa, and K. Ueda: Physica B 281&282 (2000) 465.
- [17] H. Matsui, A. Ochiai, H. Harima, H. Aoki, T. Suzuki, T. Yasuda, and N. Toyota: J. Phys. Soc. Jpn. 66 (1997) 3729.
- [18] W. Kohn: Phys. Rev. 123 (1961) 1242.
- [19] K. Koyama, M. Yoshida, T. Sakon, D. Li, T. Suzuki, and M. Motokawa: J. Phys. Soc. Jpn. 69 (2000) 3425.
- [20] M. Yoshida, K. Koyama, T. Sakon, A. Ochiai, and M. Motokawa: J. Phys. Soc. Jpn. 69 (2000) 3629.
- [21] K. Kanki and K. Yamada: J. Phys. Soc. Jpn. 66 (1997) 1103.

Figure captions:

Fig. 1:

Zero-field electrical resistivity for polydomain  $\text{Yb}_4\text{As}_3$ , plotted as  $\rho$  vs  $T$  (a) and  $\rho$  vs  $\log(T/K)$  as well as field dependence of coefficient  $A$  of the  $\rho(T,B) = \rho_0(B) + a(B)T^2$  behavior [8] (c) and coefficient of the in-T linear low- $T$  specific heat,  $\gamma(B) = C(T,B)/T$  [3] (d), normalized to their values at  $B = 0$ .

Fig. 2:

Isothermal electrical resistivity of polydomain  $\text{Yb}_4\text{As}_3$  at 2 K as  $\rho$  vs  $B^2$  (a) measured with 0.25 T/min. Arrows indicate the magnetic history of the data. The offset is due to relaxation in the resistivity  $\rho(t)$  observed at 16.5 T (b) and after driving the field back to 0 T (c). The dotted line in (c) marks the zero-field resistivity at the beginning of the cycle.

Fig. 3:

Normalized relaxation  $\rho(t)/\rho(0)$  in 16.5 T applied with a rate of 0.25 T/min at different temperatures. The different curves can be approximated by  $\rho(t)/\rho(0) = A_1 \cdot \exp(-\tau_1/t) + A_2 \cdot \exp(-\tau_2/t)$ . The inset shows the temperature dependence of the time constants  $\tau_1$  (o) and  $\tau_2$  (•).

Fig. 4:

Isothermal dc magnetization  $M$  of polydomain  $\text{Yb}_4\text{As}_3$  for magnetic fields  $B$  applied along the cubic  $\langle 111 \rangle$  direction at  $T = 2$  K, measured with a commercial SQUID magnetometer. The inset shows the time dependence  $M(t)$  vs  $t$  at 2 K after the application of 6 T.

Fig.5:

(a) Shubnikov-de Haas oscillations for magnetic fields applied parallel to the  $\langle 110 \rangle$  direction of polydomain  $\text{Yb}_4\text{As}_3$ , obtained from  $\rho(B)$  measurements in decreasing field at different temperatures. Arrows indicate maxima and minima. (b) "Landau plot" of SdH maxima (filled symbols, x-position shifted by +0.25) and minima (open symbols, x-position shifted by -0.25). The straight line has a slope of  $40 \cdot 10^{-3} \text{ T}^{-1}$ , corresponding to a SdH frequency of 25 T.

Fig. 6:

Pulsed-field resistivity  $\rho(B)$  of  $\text{Yb}_4\text{As}_3$ , measured at 0.6 K along the  $\langle 110 \rangle$  direction of polydomain  $\text{Yb}_4\text{As}_3$ , (a). SdH oscillations obtained from the 30T-pulse in decreasing field shown in (a), compared with SdH data shown in Fig. 5a (b). Vertical arrows in (a) and (b) indicate calculated positions of SdH maxima, dotted lines in (b) mark spin splitting of  $N = 1$  maximum. Fast-Fourier transformation of 30T-pulse data (c). Arrows indicate two characteristic frequencies  $F_1 = 40 \text{ T}$  and  $F_2 = 115 \text{ T}$ .

Fig. 7:

(a)  $T$ -dependence of the SdH oscillations at 7.2 T (symbols) and a fit to the standard Lifshitz and Kosevich theory (solid line). (b) Dingle-plot of  $\log(\text{amplitude} \cdot B^{1/2} \cdot \sinh(14.69 T/K \cdot m^*/m_0 \cdot T/B))$  vs  $1/B$ . From the slope of the solid lines a Dingle temperature of  $T_D = 6.6 \text{ K}$  is estimated.

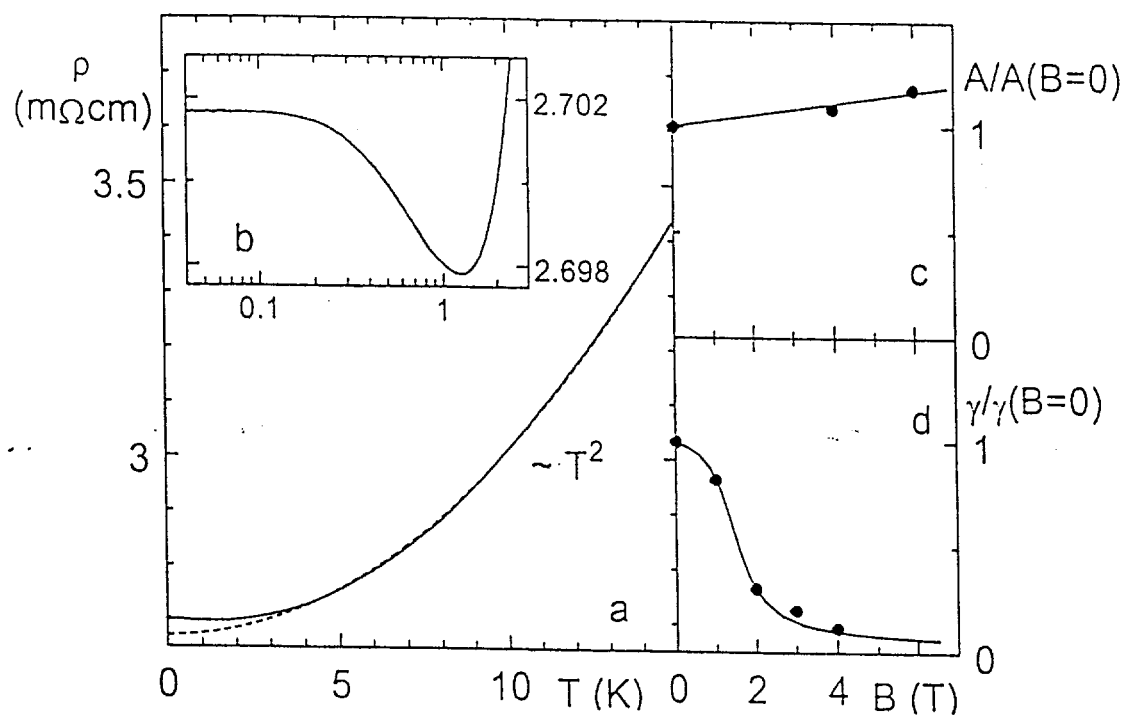


Fig. 1

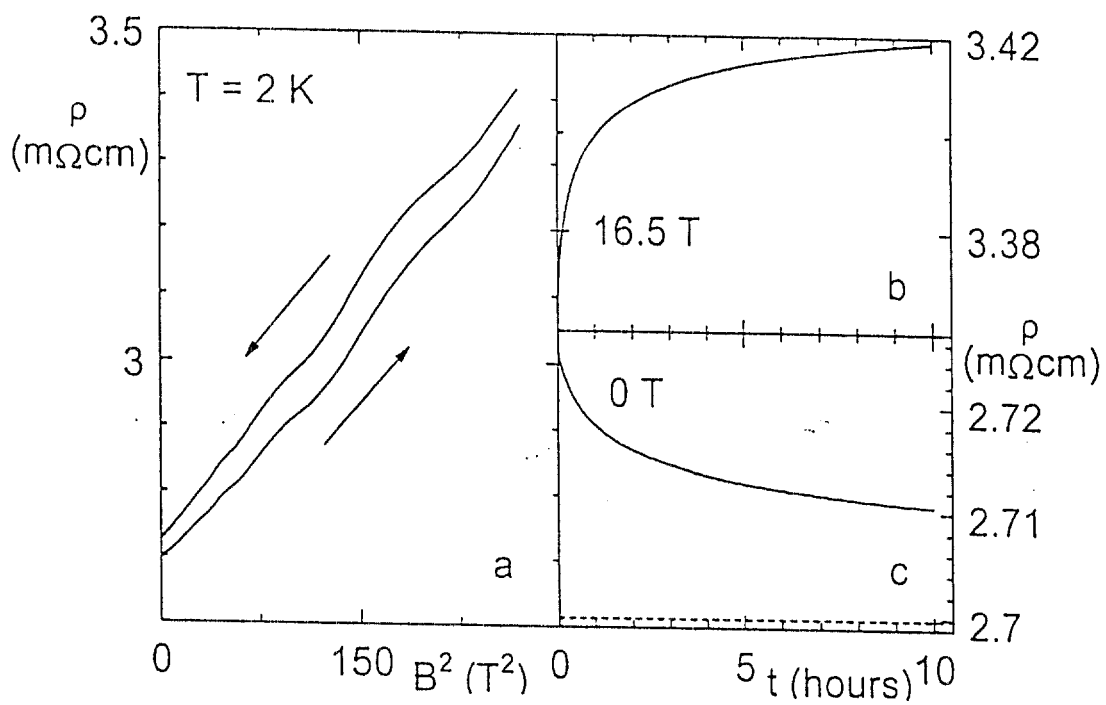


Fig. 2



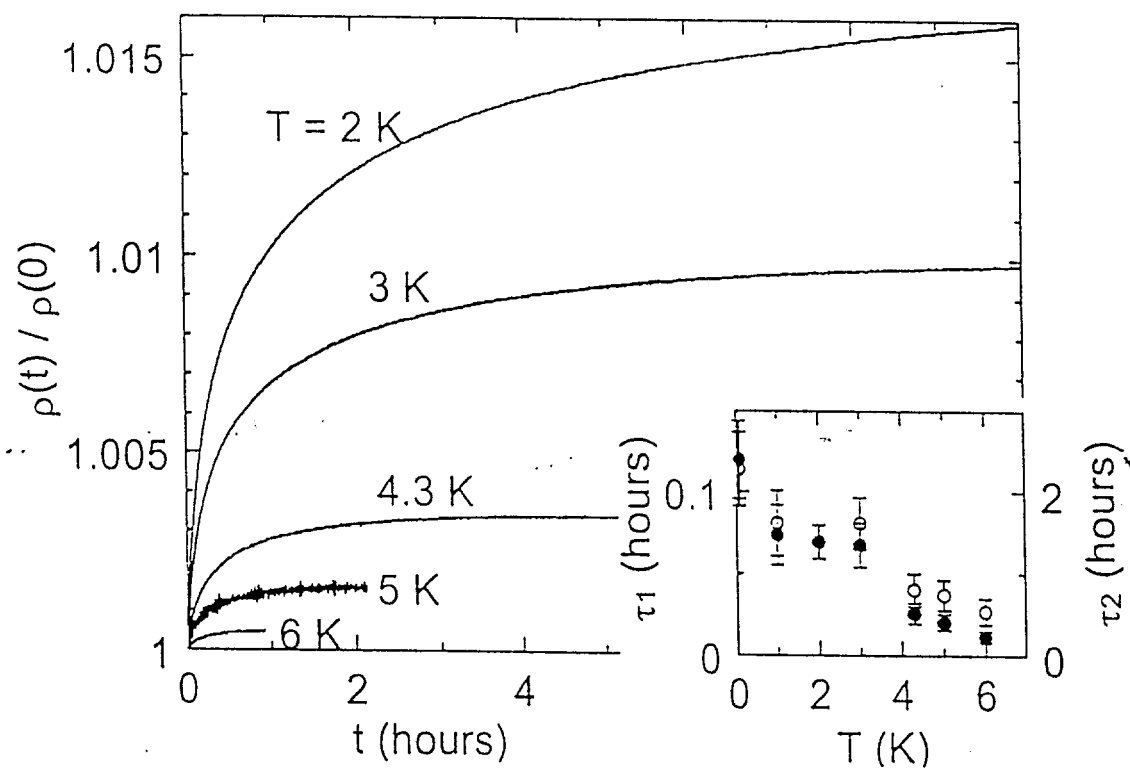


Fig. 3

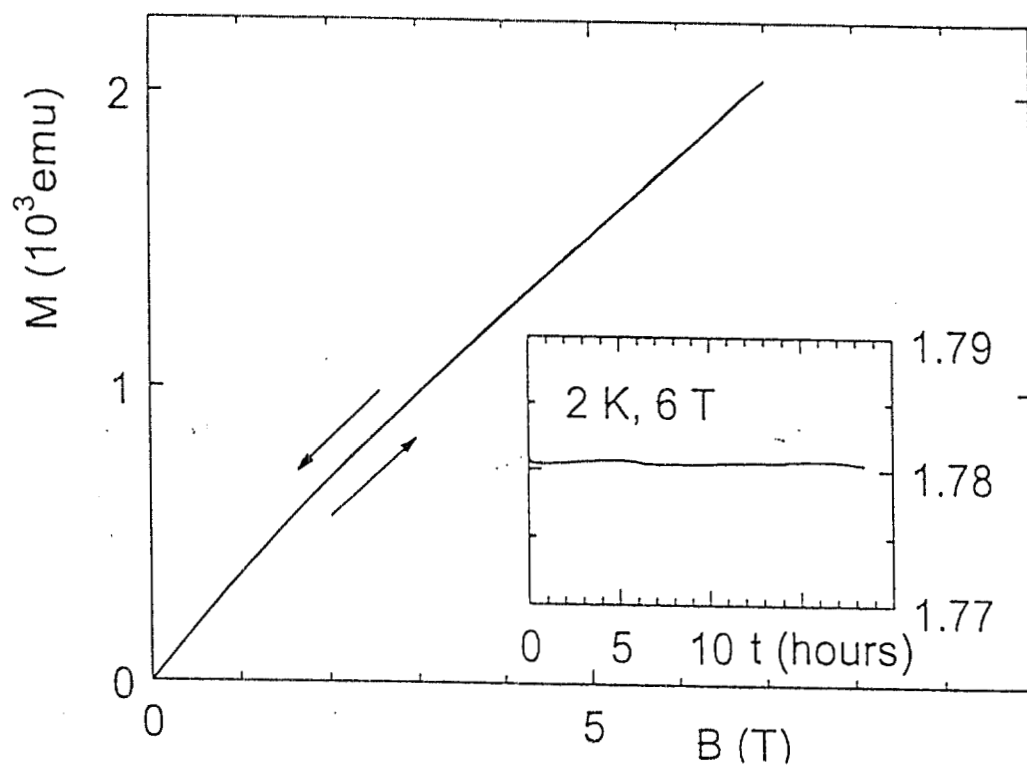


Fig. 4

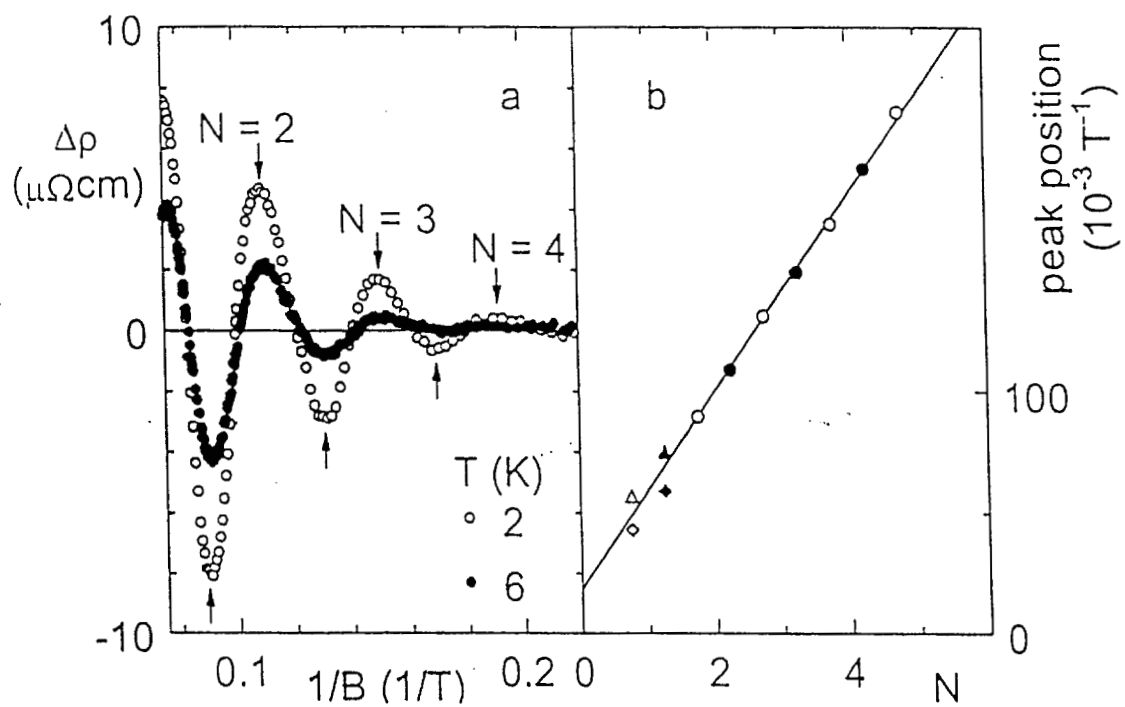


Fig. 5

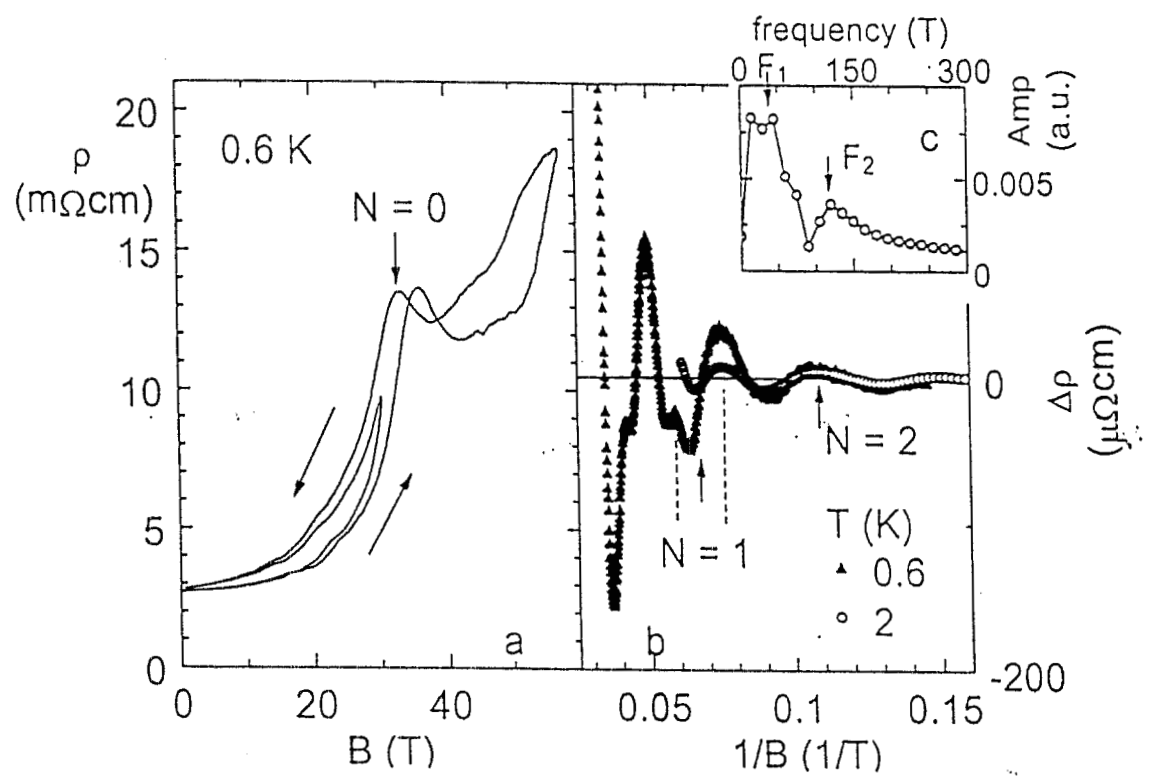


Fig. 6

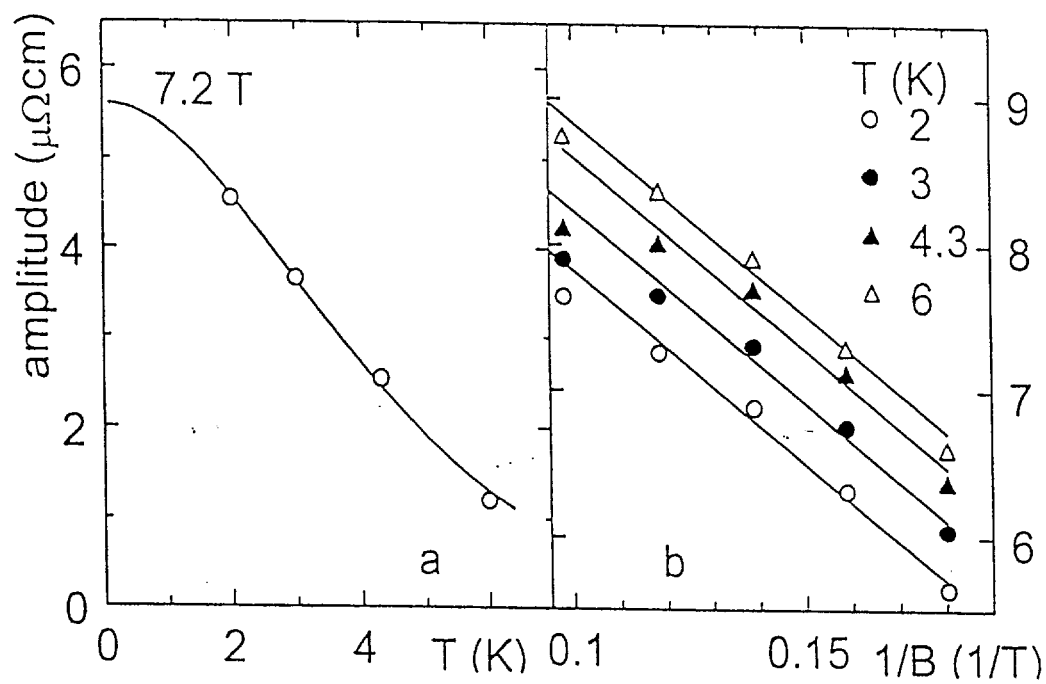


Fig. 7